Novel Chiral Pyromellitdiimide (1,2,4,5-Benzenetetracarboxydiimide) Dimers and Trimers: Exploring Their Structure, Electronic Transitions, and Exciton Coupling

Jacek Gawroński,*[a] Małgorzata Brzostowska,[a] Krystyna Gawrońska,[a] Jacek Koput,*[a] Urszula Rychlewska,*[a] Paweł Skowronek,[a, b] and Bengt Nordén[b]

Abstract: The chiral but highly symmetrical acyclic and cyclic pyromellitic diimide dimers and trimers **2**–**5** have been obtained and characterized for the first time. The pyromellitdiimide chromophores in these molecules are linked by a rigid diequatorially 1,2-disubstituted cyclohexane skeleton. The structures of the compounds have been determined in detail by molecular modeling and, in the case of cyclic dimer **4** and trimer **5**, by means of X-ray diffraction analysis. The electronically excited states of the pyromellitdiimide chromophore (**1a**) have been studied in these and other model compounds by means of linear dichroism (LD), magnetic circular dichroism (MCD), and circular dichroism (CD) spectroscopy. CD spectra of the rigid cyclic trimer **5** have provided the most detailed information on the excited states of the pyromellitdiimide chromophore. The low-energy tail (340–360 nm) of the absorption envelope can be assigned to out-of-plane polarized $n-\pi^*$ transitions (I, II). The higher energy bands are due to contributions from up to six $\pi-\pi^*$ transitions, these being polarized either along the long (IV–VI, VIII) or short axis (III, VII). The results of ab initio CIS/cc-pVDZ and semiempirical INDO/S-CI calculations have been compared with the experimental data. CD Cotton effects in the region 200–260 nm, which result from exciton interactions between electric dipole allowed transitions of two pyromellitdiimide chromophores in compounds **2**–**5**, provide reliable and useful information concerning the conformation and absolute configuration of these molecules, which may be extrapolated to other oligoimide systems.

Keywords: chirality · circular dichroism · electronic transitions · pyromellitic diimides

Introduction

Diimides of 1,2,4,5-benzenetetracarboxylic acid (abbreviated herein as pyromellitdiimides) constitute a group of heteroaromatic compounds of ever increasing importance in organic, biological, and medicinal chemistry, as well as in physical, supramolecular, and materials chemistry. Pyromellitdiimides are widely used as rigid structural components, for example in catenanes[1] and in clathrate hosts.[2] The use of pyromellitdiimides as acceptors in various electron-transfer and photosynthetic charge-separation systems,[3] often in conjunction with porphyrin derivatives,[4–8] has presented a considerable challenge and has been extensively studied.

[a] Prof. Dr. J. Gawroński, Prof. Dr. J. Koput, Prof. Dr. U. Rychlewska, Dr. M. Brzostowska, Dr. K. Gawrońska, Dr. P. Skowronek
Department of Chemistry, A. Mickiewicz University
Grunwaldzka 6, 60780 Poznań (Poland)
Fax: (+48) 68-865-8008
E-mail: gawronsk@amu.edu.pl

[b] Dr. P. Skowronek, Prof. Dr. B. Nordén
Department of Physical Chemistry
Chalmers University of Technology
41296 Göteborg (Sweden)

Surprisingly, the excited states of the pyromellitdiimide chromophore have not been studied in any detail, despite their relevance to the widely investigated photoelectron transfer and nonlinear optical properties. Recently, we presented a preliminary report on exciton coupling between various types of aromatic imides, including pyromellitdiimide, in which we demonstrated their utility in making stereochemical assignments.[9] Previously, we have shown that the structurally related phthalimide is an excellent chromophore for determining absolute configuration[10, 11] and conformation,[12] based on exciton coupling of the allowed long-axis polarized $\pi-\pi^*$ transition. These applications were extended to *N*-phthaloyl derivatives of amino acids[13] and allylic amines,[14] while others used 2,3-naphthaloyl derivatives of amines to make configurational assignments.[15]

To obtain a more complete picture of the electronic transitions and their polarizations in the pyromellitdiimide chromophore, we have applied the linear dichroism (LD) and magnetic circular dichroism (MCD) techniques to monomeric diimide **1b**, which is more soluble than the parent pyromellitdiimide **1a**. Circular dichroism (CD) measurements are often more sensitive than isotropic absorption (UV) measure-

  0947-6539/02/0811-2484 $ 20.00+.50/0

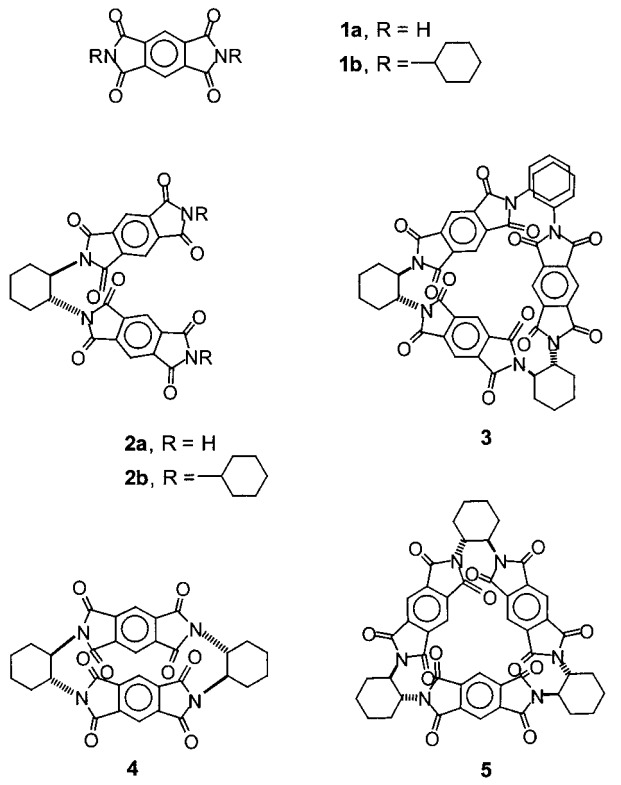

Abstract in Polish: *Po raz pierwszy zostały otrzymane i scharakteryzowane chiralne lecz wysoce symetryczne acykliczne i cykliczne dimery i trimery **2**–**5** diimidu piromelitowego. W tych cząsteczkach chromofory piromelitowe są połączone przy pomocy sztywnego 1,2-diekwatorialnie podstawionego szkieletu cykloheksanu. Szczegółowe struktury tych związków zostały określone za pomocą modelowania molekularnego, a w przypadku cyklicznego dimeru **4** i trimeru **5**, także za pomocą dyfrakcji promieni rentgenowskich. Zbadano elektronowe stany wzbudzone chromoforu piromelitowego tych i innych modelowych cząsteczek, stosując pomiary dichroizmu liniowego (LD), magnetycznego dichroizmu kołowego (MCD) oraz dichroizmu kołowego (CD). Widma CD sztywnego cyklicznego trimeru **5** dostarczyły najbardziej szczegółowych informacji dotyczących stanów wzbudzonych chromoforu piromelitowego. Niskoenergetyczna część (340–360 nm) widma absorpcyjnego została przypisana przejściom n–π* (I, II) spolaryzowanym poza płaszczyzną. Pasma absorpcyjne o wyższej energii są spowodowane udziałami aż do sześciu przejść π–π* spolaryzowanych wzdłuż osi podłużnej (IV–VI, VIII) lub poprzecznej (III, VII) cząsteczki. Porównano wyniki obliczeń stanów wzbudzonych metodami ab initio CIS/cc-pVDZ i semiempirycznymi INDO/S-CI z danymi doświadczalnymi. Efekty Cottona w zakresie 200–260 nm we widmie CD, które wynikają z oddziaływań ekscytonowych między elektrycznie dipolowo dozwolonymi przejściami dwóch chromoforów piromelitowych w związkach **2**–**5**, dostarczyły użytecznych i o dużej pewności informacji o konformacji i absolutnej konfiguracji tych cząsteczek, z możliwościami zastosowań w innych systemach oligoimidowych.*

ments for detecting hidden electronic transitions, and for this purpose we chose a series of highly symmetrical yet chiral dimeric (**2**, **4**) and trimeric (**3**, **5**) pyromellitdiimides incorporating (*R*,*R*)-*trans*-1,2-diaminocyclohexane as a linker. This linker not only provides a chiral environment enabling circular dichroism studies of the dimers and trimers, but also a well-defined structure in which the cyclohexane substituents rigorously occupy the equatorial positions. As expected, the cyclic oligomers **4** (D_2) and **5** (D_3) differ from the acyclic ones **2** (C_2) and **3** (C_2) in terms of the degree of rigidity: while there is some rotational freedom about the individual pyromellitdiimide longitudinal symmetry axes in **2** and **3**, no such rotation is anticipated at ambient temperatures in the rigid structures **4** and **5**. It was anticipated that the rigid structures of **4** and **5** would display more pronounced Cotton effects than **2** and **3**, as the CD in these last two compounds tends to cancel out to a high degree due to rotational averaging.[16] The structures of the dimers and trimers were established by computational (DFT or AM1), spectroscopic (NMR), and X-ray diffraction methods. Computations of the excited states of **1a**, **2a**, and **4** were carried out at the ab initio CIS/cc-pVDZ level, and the results were compared with those from INDO/S-CI calculations as well as with the experimental data.

Results and Discussion

Structure and properties: The dimeric and trimeric pyromellitdiimides **2b**–**5** are high-melting solids, soluble in nonpolar organic solvents (e.g., dichloromethane, benzene). This enables their ready separation, purification, and spectroscopic analyses.

Molecular modeling of **2b** (AM1) yielded a low-energy structure of C_2 symmetry, which could be best characterized by two torsion angles, ω_1 H-C-N-C(O) and ω_2 N-C-C-N (Figure 1). The first of these indicates rotation of the

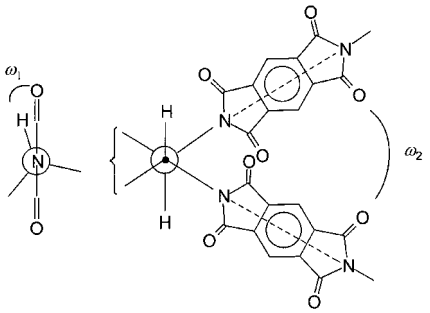

Figure 1. Torsion angles determining the structures of **2**–**5**.

pyromellitdiimide plane out of coplanarity with the (N)C–H bond, a structural feature common to many aromatic imides, such as phthalimides,[11] derived from amines attached to a disubstituted carbon atom. The second torsion angle (ω_2) defines the noncoplanarity of the longitudinal symmetry axes, which bisect the pyromellitic nitrogen atoms in the two vicinal imide chromophores. The sign and magnitude of this angle plays a decisive role in determining the chiroptical properties of pyromellitic dimers and trimers (see below).

  0947-6539/02/0811-2485 $ 20.00+.50/0

As listed in Table 1, in the case of **2b**, the computed values of these two torsion angles are $\omega_1 = -2.4^\circ$ and $\omega_2 = -53.7^\circ$ (C_2 symmetry), which are typical for a strain-free cyclohexane ring with vicinal imide substituents in the equatorial positions.[9] The value of ω_1 is, however, different from those (9.8° and 15.9°) measured for a bis(phthaloyl) derivative of (*R*,*R*)-1,2-diaminocyclohexane by X-ray diffraction analysis.[11]

Table 1. Calculated and X-ray diffraction determined torsion angles for oligomers **2**–**5**.

	ω_1 (H-C-N-C) [°][a]	ω_2 (N-C-C-N) [°]
2a[b]	−2.8	−58.9
2b[c]	−2.4	−53.7
3*C*[c]	−5.1; −3.4	−53.9
3*S*[c]	−5.1; −3.4	−53.9
4[d]	−3.2; −0.1	−44.3; −44.0
4[e]	2.3; −3.2	−42.4
	−1.7; −2.5	−42.7
5[f]	16.3	−50.1
5[g]	12.2; 16.1	−49.8

[a] Two values separated by a semicolon refer to two H-C-N-C angles originating from the same cyclohexane ring. [b] Calculated (B3LYP/cc-pVDZ) for a molecule of C_2 symmetry. [c] Calculated (AM1) for a molecule of C_2 symmetry. [d] Calculated (AM1; B3LYP/cc-pVDZ) for a molecule of D_2 symmetry. [e] Determined by X-ray crystallography for two independent molecules. [f] Calculated (AM1) for a molecule of D_3 symmetry. [g] X-ray determined for a molecule of C_3 symmetry.

The case of trimer **3** is different in that two diastereomeric conformers can be envisaged. Their structures, designated with the letters *C* and *S*,[17] are shown in Figure 2. Their computed (AM1) heats of formation are equal to within 0.3 kcal mol^{-1}, and hence nearly equal equilibrium populations of the two conformers can be assumed.

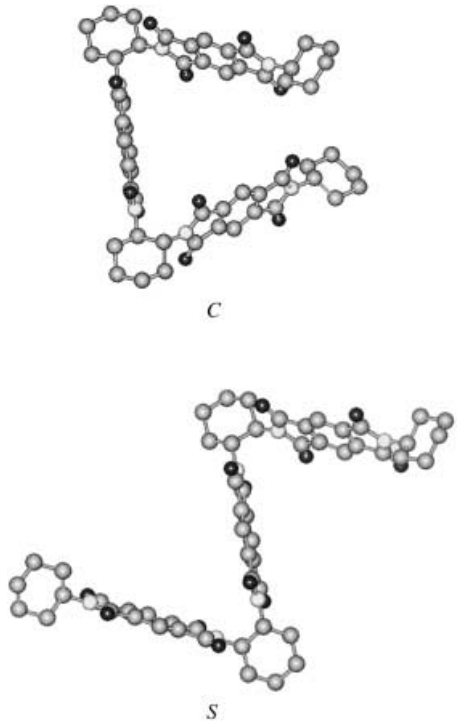

Figure 2. Low-energy conformers of **3** from AM1 computation. Conformers *C* and *S* are *M* and *P* helical, respectively.

The presence of the two conformers in equilibrium is clearly evident in the ^{1}H NMR spectra of **3**. Whereas the aromatic protons of **3** give rise to broad overlapping signals at 293 K (Figure 3), they are seen as sharp singlets upon lowering the temperature of measurement to 253 K. A maximum of three aromatic proton signals of equal intensity

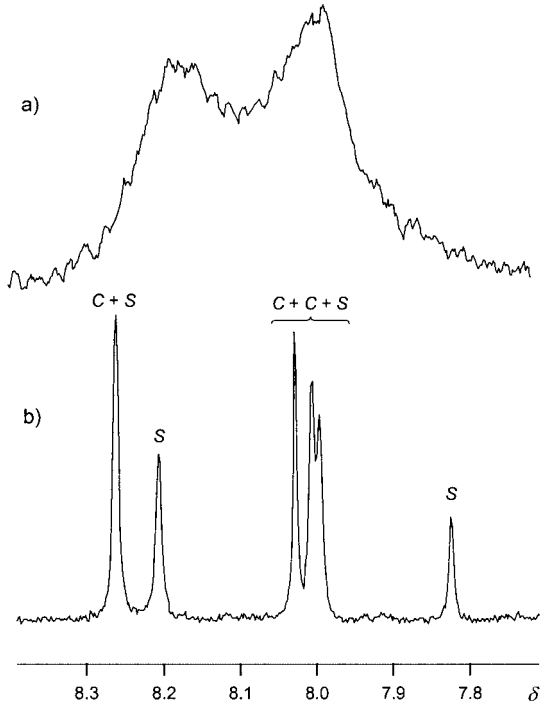

Figure 3. Aromatic region ^{1}H NMR spectra of **3** in $CDCl_3$: a) at 293 K, b) at 253 K.

can be expected for conformer *C*, due to the magnetic equivalence of the protons of the central pyromellitdiimide molecule, while four signals in a 1:2:2:1 intensity ratio can be expected for conformer *S* of **3**. In practice, only six signals were observed at 253 K, due to degeneracy of the two of the resonance signals, the superimposed signal appearing as a three-proton singlet at $\delta = 8.28$.[18] The position of the one-proton signal at $\delta = 7.86$ is noteworthy. The upfield shift of this signal is due to deshielding of one of the protons of the central pyromellitdiimide unit by *both* outer pyromellitdiimide molecules. Significantly, analysis of the intensities of the NMR signals leads to the conclusion that both conformers of **3** are essentially equally populated under the measurement conditions.

The torsion angles ω_1 and ω_2 computed for each of the conformers of **3** are shown in Table 1. As expected, the values of ω_1 and ω_2 are practically identical and are not significantly different from those computed for the dimer **2b**.

Cyclic dimeric pyromellitdiimide **4** is the only highly strained molecule examined in this study. Molecular modeling (AM1) and ab initio B3LYP computation (Table 1) provide structures that are very close to that determined by X-ray diffraction analysis of the crystal (see below) and which accommodate the strain due to formation of a cyclic structure by [2+2] cyclocondensation of *trans*-1,2-diaminocyclohexane

  0947-6539/02/0811-2486 $ 20.00+.50/0 *Chem. Eur. J.* **2002**, *8*, No. 11

and pyromellitic dianhydride. The strain is manifested in several structural features, such as a bending of each of the pyromellitdiimide moieties (Figure 4) and a change in the values of the angles ω_1 and ω_2 compared to those of **2b** (Table 1). The computed angle ω_1 in **4** is small ($-3.2^\circ/-0.1^\circ$) and the cyclohexane ring is flattened so that the torsion angle ω_2 is decreased to $-44.3^\circ/-44.0^\circ$. The ^{1}H NMR spectrum of **4** displays only a sharp singlet due to the aromatic protons at $\delta = 7.86$, indicative of high symmetry (point group D_2) and restricted conformational mobility of the molecule.

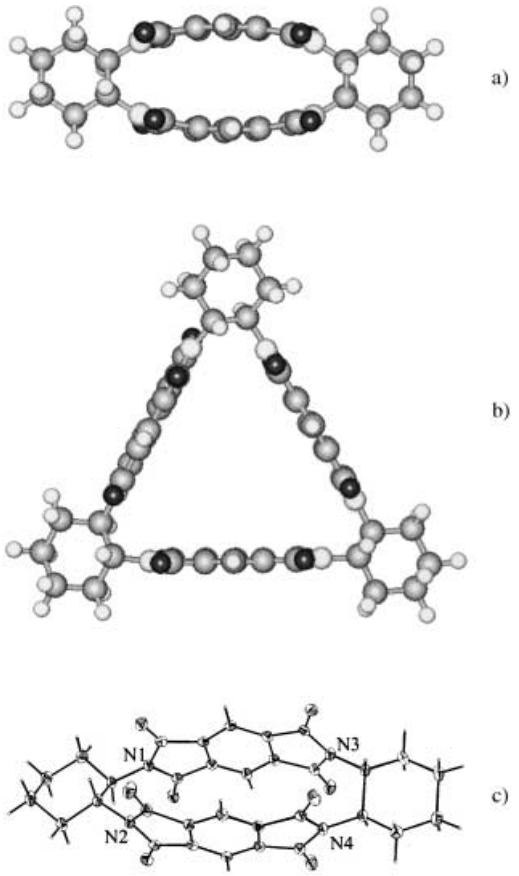

Figure 4. AM1 computed minimum energy structures of **4** (a) and **5** (b), as well as a perspective view of the X-ray determined structure of **4** (c). Thermal ellipsoids are drawn at a 40% probability level and give a graphical representation of atomic displacements at 150 K.

Cyclic trimeric pyromellitdiimide **5** forms a strain-free structure, with planar imide moieties at the sides and the cyclohexane rings at the apices of the triangle (Figure 4). Similar regular triangular hexaimine structures have recently been reported as products of the reactions of *trans*-1,2-diaminocyclohexane with aromatic dialdehydes.[19–21] The AM1 computed ω_1 and ω_2 angles for D_3-symmetrical molecule **5** (Table 1) are 16.3° and -50.1°, which are only slightly different from the corresponding values obtained by X-ray diffraction analysis of the crystal (see below). In accordance with the highly symmetrical and rigid structure, the aromatic protons give rise to a sharp singlet at $\delta = 8.04$ in the ^{1}H NMR spectrum of **5**.

X-ray structures and inclusion properties of 4 and 5: We were unable to obtain crystals of **3** suitable for X-ray analysis and therefore to determine which of the two conformers (*C* or *S*) is the preferred one in the solid state. The two other compounds of interest with regard to X-ray structure determination, the cyclic dimer **4** and the cyclic trimer **5**, were studied as co-crystals with benzene solvent molecules and form various types of inclusion compounds. The molecule of **4** is shown in Figure 4.[22] The asymmetric unit (in the case of the *P*1 space group this is also the whole unit cell) contains one molecule of **4** and one molecule of the benzene solvent. Although there are no symmetry constraints linking any set of distances and angles in the potentially symmetrical molecule of **4**, the two parts of the dimer are very much alike and their geometry is nearly identical to that observed in pyromellitdiimide molecules[23, 24] as well as their *N*,*N*′-dialkyl derivatives.[25, 26] As expected, the formation of dimeric species occurs with a loss of planarity of the two pyromellitdiimide moieties, which are bent towards each other. The root-mean-square deviations of atoms defining the two fragments are 0.159 and 0.160 Å, with the mean standard uncertainty of the individual atomic deviations equal to 0.002 Å. If one defines the best least-squares plane through the atoms constituting the six-membered ring, the remaining atoms of the pyromellitdiimide fragment are all displaced in one direction: positive for one pyromellitdiimide moiety and negative for the other. We have chosen to describe the geometry of each of the two fragments in terms of two least-squares planes, each defined by five atoms forming the imide ring. The angle between the planes containing nitrogen atoms N1 and N3, which we take as the fold angle of the pyromellitimide fragment, is 20.24(9)°. The analogous angle between the planes containing nitrogen atoms N2 and N4 is equal to 20.44(9)°. The sums of the valence angles around the nitrogen atoms (358.5, 356.6, 356.8, and 358.5° for N1 to N4, respectively) indicate slight pyramidalization at nitrogens N2 and N3. Both cyclohexane rings adopt a conformation close to an ideal chair form. The average torsion angle magnitude is the same in the two rings, amounting to 58.3°. This value is somewhat higher than that quoted for a cyclohexane ring in ideal chair form, 54.9°,[27] reflecting significant ring puckering. An increase in the endocyclic torsion angle at the site of substitution to values of 63.5(3)° and 61.5(3)° causes a decrease in the torsion angle between the *trans*-diequatorially oriented nitrogen atoms. The values of the N-C-C-N torsion angles are $-42.4(3)^\circ$ and $-42.7(3)^\circ$.

Figure 5 shows a packing diagram. Along the *x* axis, the molecules are arranged in such a way that we observe both intra- and intermolecular stacking interactions between their flat parts. The perpendicular distance between the plane of the six-membered carbocyclic ring and the midpoint of its intramolecular analogue is 3.586 Å, while the corresponding distance to the intermolecular equivalent is 3.217 Å. The angle between the interacting six-membered rings is equal to 2.8° and the rings are mutually twisted by 9.6°, inducing a helical twist (the twist angle is measured as the angle between lines connecting the atoms in the *para* positions). Within the dimer, the mutual shift of the interacting planes is negligible (0.306 Å), but the intermolecularly interacting partners are

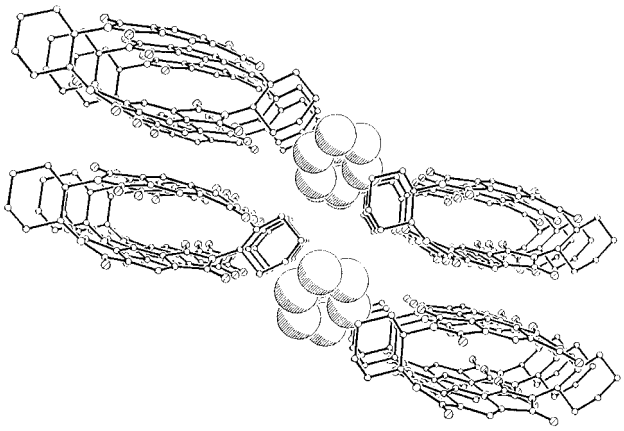

Figure 5. Packing of the molecules of **4** as viewed down the *y* axis. Carbon atoms of the benzene solvent molecules are represented as van der Waals spheres of radius 1 Å.

shifted with respect to each other by 1.563 Å. Translationally related along the *y* axis, the molecules of **4** form an edge-on pile, resulting in microporous columns within which the molecules are connected by C–H···O hydrogen bonds. Combined with planar stacking along the *x* axis, the arrangement of molecules in the (001) plane resembles a wall with numerous microporosities. Benzene solvent molecules separate molecules that are neighbors along the *z* axis. Translationally related along the *x* axis, the solvent molecules are arranged in channels formed by the cyclohexane rings. They are connected to the molecules of **4** along the *z* axis by means of C–H···O and C–H···π hydrogen bonds.

The arrangement of the molecules of **5** and the benzene solvent molecules in the crystal is illustrated in Figure 6. The asymmetric unit contains one-third of the molecule of **5**, which is located on a threefold axis, and three fragments constituting one-third of the benzene solvent molecule: two such fragments are situated on a threefold axis and one on a sixfold screw axis. Potentially highly symmetric (D_3 symmetry), in the crystal the molecule of **5** shows only C_3 symmetry. In contrast to **4**, the pyromellitimide moiety is planar, the root-mean-square deviation of the atoms defining the fragment being only 0.047 with the mean standard uncertainty of the individual atomic deviations equal to 0.002 Å, and the angle between the best planes through the imide rings being only 5.80(9)°. The sums of the valence angles about the nitrogen atoms are equal to 358.9(2)° and 360.0(2)°, indicating planar configurations. The cyclohexane ring adopts a conformation very similar to that observed in **4**, with the average torsion angle magnitude being 57.8° and significant ring puckering at the site of substitution (the C6-C1-C2-C3 and N-C-C-N torsion angles amount to 60.9(3)° and −49.8(3)°, respectively).

A characteristic of the crystal packing of the trimer **5** is that the benzene solvent molecules are arranged in layers parallel to the (001) plane at approximately 0 and 1/2 *z* level, with the molecules of **5** in between these layers (Figure 6). Two of the three benzene solvent molecules are situated on a threefold axis, and one on a 6_3 screw axis. The molecules situated on a threefold axis are subject to static disorder. These solvent molecules are situated above and below the molecular

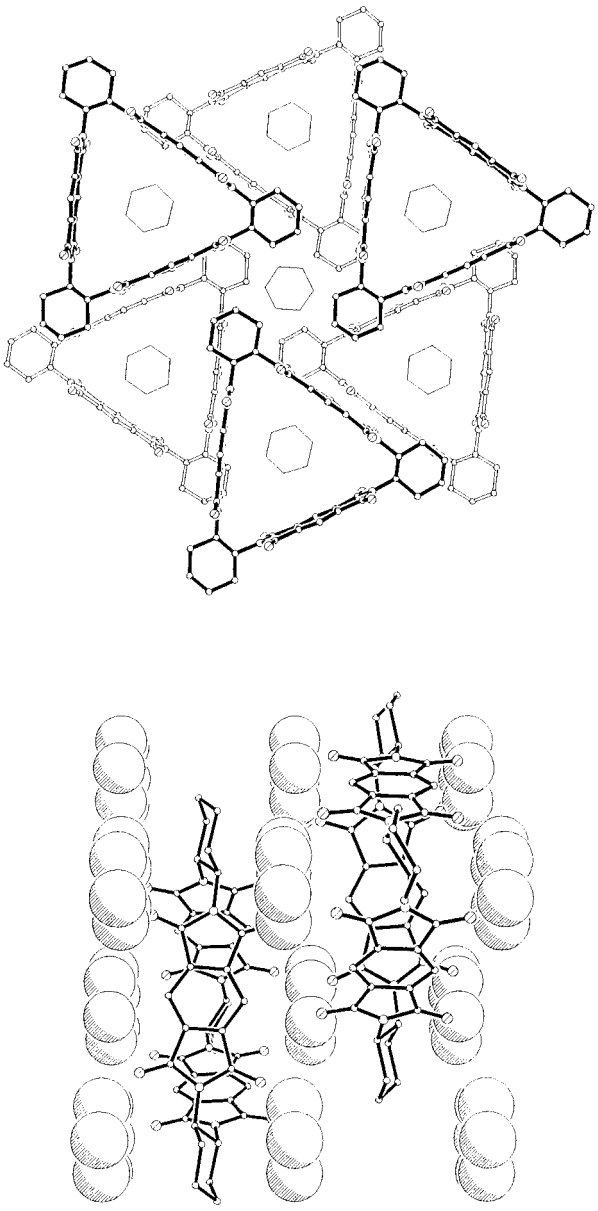

Figure 6. Part of the crystal structure of **5**. The benzene solvent molecules lie on three 6_3 and symmetry axes. Only the major orientation of the disordered benzene molecules lying on a threefold axis is shown. Top: View down the *z* axis showing three consecutive (001) layers, differentiated by thick, thin, and open lines. Bottom: Side view of the (001) layers. Carbon atoms of the benzene solvent molecules are represented as van der Waals spheres of radius 1 Å.

triangle, giving the impression that they are trying to enter the void inside the pyromellitdiimide trimer but without any success.

Electronic transitions and circular dichroism—exciton coupling: The UV isotropic absorption spectrum of *N*,*N*′-dicyclohexyl pyromellitdiimide (**1b**) consists of two regions (Figure 7). The low-intensity (ε below 3000 $mol^{-1}\,dm^3\,cm^{-1}$) region from about 380 nm to 280 nm is dominated by a π–π* transition polarized in the *z* direction (see Table 2 for polarization directions).[9] The intense absorption region 280–200 nm is also dominated by a *z*-polarized π–π*

  0947-6539/02/0811-2488 $ 20.00+.50/0 *Chem. Eur. J.* **2002**, *8*, No. 11

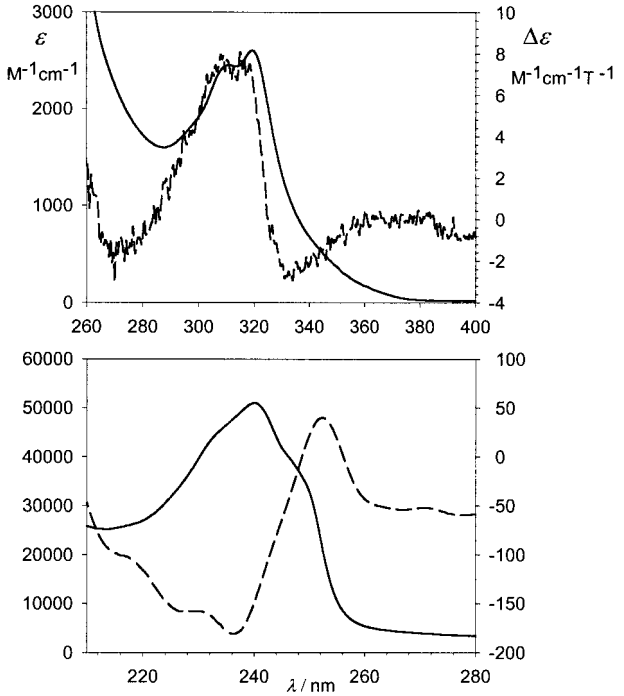

Figure 7. UV isotropic absorption (solid line) and magnetic circular dichroism (dashed line) spectra of **1b** in dioxane.

transition, as predicted by an INDO/S calculation.[9] However, the electronic absorption spectrum of **1a** is evidently composed of a number of other bands in both regions, which are not sufficiently resolved.

Magnetic circular dichroism spectra are often used to resolve the transitions that contribute to the absorption bands under study. In the case of the pyromellitic chromophore of **1b**, for which the ground and the excited states are non-degenerate, we would expect to observe a B-type spectrum in which nearly orthogonally polarized transitions appear as sign-reversed MCD signals.[28] In the low-energy absorption region (Figure 7, top panel), we indeed observe a bisignate MCD signal, quite similar in shape to that of the phthalimide chromophore.[11] The corresponding weak UV band appears on the slope of a much stronger absorption at higher energy, and it shows a maximum at 319 nm and a shoulder at about 310 nm. The two transitions, although poorly resolved in the UV spectrum, have opposite transition polarizations, which accordingly can be assigned as z and y (bands III and IV in Table 2). In the higher-energy region (lower panel in Figure 7), the B-term MCD signal is also evident, corresponding to the shoulder at about 248 nm and the maximum at 240 nm. The two transitions are orthogonally polarized, accordingly in the y and z directions, and are labeled as bands VI and VII (Table 2).

The UV absorption and reduced linear dichroism (LD^r) spectra of *N*,*N*′-dicyclohexyl pyromellitdiimide (**1b**) oriented in a stretched PVC film are shown in Figure 8. Due to only partial orientation of the imide molecules, the amount of information available from the experiment is somewhat limited (use of poly(vinyl alcohol) or polyethylene stretched films for sample orientation did not provide better results). Assuming C_{2v} symmetry of the chromophore and a rod-like orientation in the stretched PVC film,[29] as in the case of phthalimides,[11] we could assign a long axis (z) polarized $\pi-\pi^*$ transition (band III in Table 2) to the observed maximum at around 320 nm in the LD^r spectrum. Likewise, the LD^r minimum at 290 nm may correspond to the y-polarized $\pi-\pi^*$ transition (band IV in Table 2), overlapping with another very weak transition at 270 nm (band V). Below

Table 2. Observed and calculated electronic transitions of pyromellitdiimides.

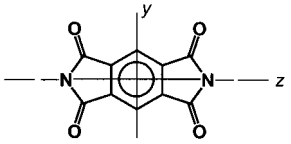

	Experimental, **1b** and **5**			INDO/S **1a**			CIS/cc-pVDZ **1a**		
Band	λ [nm]	ε [$M^{-1}cm^{-1}$][a]	Pol.[b]	Symm.[c]	λ [nm][d]	f[d]	Symm.[c]	λ [nm][e]	f[e]
I	355[f]	–	–	B_{3u} n → π*	379	0.002 (x)	B_{2u} π → π*	329	0.04 (y)
				B_{2g} n → π*	375	0	B_{3u} n → π*	324	0.002 (x)
II	340[f]	–	–	B_{1g} n → π*	359	0	B_{1u} π → π*	319	0.09 (z)
				A_u n → π*	356	0	B_{2g} n → π*	318	0
III	319	2600	z	B_{1u} π → π*	296	0.05 (z)	B_{1g} n → π*	297	0
IV	310	2450	y	B_{2u} π → π*	275	0.1 (y)	A_u n → π*	295	0
V	270[f]	–	y	B_{3g} π → π*	234	0	B_{2u} π → π*	246	0.008 (y)
VI	≈248; 250[f]	shoulder	y	B_{2u} π → π*	222	0.5 (y)	B_{3g} π → π*	243	0
VII	240	51000	z	B_{1u} π → π*	223	1.4 (z)	B_{1u} π → π*	240	1.6 (z)
				B_{3u} n → π*	216	0.00009 (x)	B_{2u} π → π*	224	1.4 (y)
				B_{3g} π → π*	214	0	B_{3g} π → π*	216	0
				A_u n → π*	211	0	A_u n → π*	212	0
				B_{1g} n → π*	209	0	A_g π → π*	200	0
				B_{2g} n → π*	205	0	B_{3u} n → π*	198	0.003 (x)
VIII	≈232; 215[f]	shoulder	y	B_{2u} π → π*	202	0.5 (y)	B_{1g} n → π*	192	0

[a] UV absorbances of **1b** in acetonitrile. [b] Polarization of transitions from either LD or MCD of **1b**; see formula above for the definition of the molecular coordinate system. [c] Symmetry of the excited state in the D_{2h} point group and the transition type. [d] Transition wavelength (λ) and oscillator strength (f) calculated by the INDO/S method (transition moment polarization along the fixed axes of the molecule is given in parentheses; x: out-of-plane, y: short axis, z: long axis). [e] Transition wavelength (λ) and oscillator strength (f) calculated at the CIS/cc-pVDZ level of theory. The computed wavelengths were multiplied by a scaling factor of 1.4 (see text). [f] CD of **5** in acetonitrile.

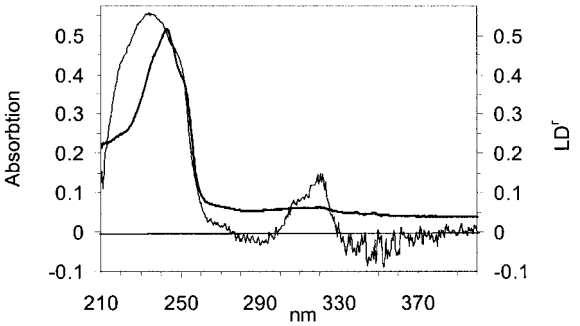

Figure 8. UV isotropic absorption (thick line) and reduced linear dichroism (thin line) spectra of **1b** in a stretched PVC film at 293 K.

260 nm, the LD^r bands are poorly resolved and the only assignment that can be made with confidence is that of the LD^r maximum at 235 nm, corresponding to the strong, *z*-polarized $\pi-\pi^*$ transition with a maximum at 240 nm (band VII).

The CD spectra of chiral diimide dimers (**2b**, **4**) and trimers (**3**, **5**) were investigated next. For the bichromophoric system having a negative ω_2 torsion angle (Figure 1 and Table 1), negative exciton-split Cotton effects were to be expected for the pyromellitic chromophore long-axis (*z*) polarized $\pi-\pi^*$ transitions. In the case of **2b** (Figure 9), a weak negative

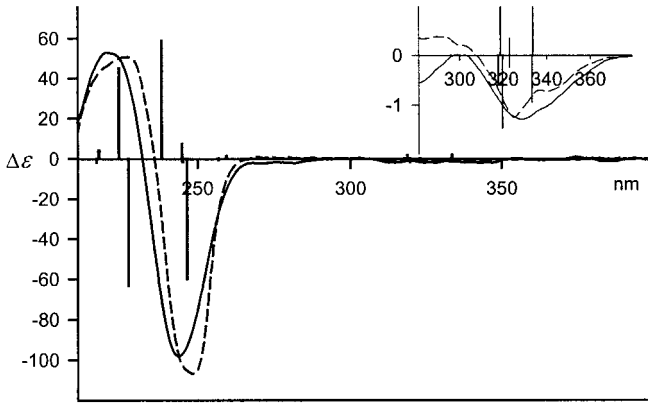

Figure 9. CD spectra of **2b** (dashed line) and **3** (solid line) in dioxane at 293 K, sample concentration approximately 1.5×10^{-4} M. The ab initio calculated CD spectrum of **2a** is inserted as a stick diagram.

Cotton effect ($\Delta\varepsilon$ −1.2) is observed at 325 nm, which corresponds to the *z*-polarized transition III in Table 2. A weak shoulder is seen at 340 nm, apparently due to an $n-\pi^*$ transition II. At shorter wavelengths, a pair of strong Cotton effects is seen, $\Delta\varepsilon$ −106.7 at 248 nm and $\Delta\varepsilon$ 50.7 at 227 nm, undoubtedly due to the coupling of the electric dipole transition moments of the intense, *z*-polarized transition VII ($\varepsilon=90000$ at 238 nm). This band is slightly (2 nm) blue-shifted relative to the position of λ_{max} for monomer **1b**, as one would expect for a system of two inclined noncoplanar electric dipole transition moments.[30]

The case of **3** is more complex. As discussed above, in solution the trimeric diimide **3** exists as a mixture of two nearly equally populated conformers *C* and *S* (Figure 2), which can be distinguished by ^{1}H NMR spectroscopy. The CD spectrum of **3** is therefore an average of the CD spectra of these *C* and *S* conformers. The computed geometries of both the *C* and *S* conformers of **3** (Table 1) show a high degree of similarity to the geometry of the component molecule **2b**. Thus, the torsion angles ω_1 and ω_2 are similar for **2b**, **3***C*, and **3***S*, the only discrepancy being the existence of two different values of ω_1 in each conformer of **3**. The slightly lower value of ω_1 (−3.4°) was computed for the two inner H-C-N-C(O) bond systems, whereas the value of −5.1° corresponds to the two outer H-C-N-C(O) bond systems in **3**. The CD of the trimer can be treated as the sum of Cotton effects due to exciton coupling of each constituent chromophoric pair; in other words, it includes two dimer Cotton effects as the first term and Cotton effects due to 1,3-bichromophoric interactions as the second term. Since the first term will dominate, the CD of **3** should be quite similar to that of **2b** (excluding differences in the magnitudes of the Cotton effects). In practice, the CD spectra of **2b** and **3** are indeed almost identical (Figure 9), save for small differences in intensity and a blue shift of the Cotton effects of trimer **3** compared to those of **2b**. In the case of **3**, the pair of intense $\pi-\pi^*$ Cotton effects appears at 244 nm ($\Delta\varepsilon$ −98.1) and 220 nm ($\Delta\varepsilon$ +53.0).

Diimide ring distortion in cyclic dimer **4** is clearly manifested in the UV and CD spectra (Figure 10).

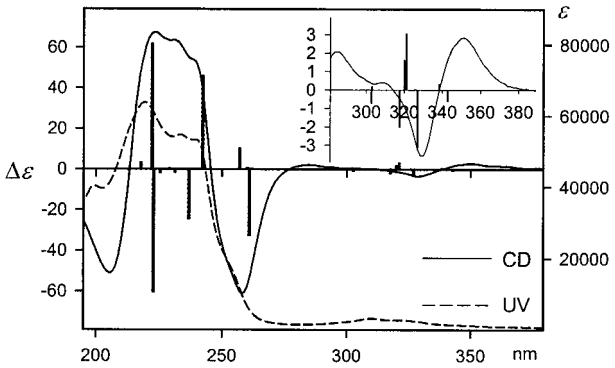

Figure 10. CD and UV spectra of **4** in acetonitrile (conditions as for Figure 9). The ab initio calculated CD spectrum of **4** is inserted as a stick diagram.

These spectra are very different from those of the corresponding acyclic dimer **2b** and the monomer **1b**. The UV bands below 260 nm are better resolved: shoulders are seen at 254 nm and 239 nm, as well as maxima at 233 nm and 219 nm, the latter due to the most intense transition in **4** ($\varepsilon=63700$). The shoulder at 254 nm in the UV spectrum corresponds to the intense CD band at 258 nm ($\Delta\varepsilon$ −60.9). The other three transitions in the CD spectrum are resolved, appearing as a negative couplet (a shoulder at about 250 nm and a maximum at 240 nm), a positive maximum at 230 nm ($\Delta\varepsilon$ +63.7), and a positive couplet (a maximum at 223 nm, $\Delta\varepsilon$ +67.5, and a minimum at 205 nm, $\Delta\varepsilon$ −50.8). In the region above 300 nm, two distinct Cotton effects are evident: a positive one ($\Delta\varepsilon$ +2.8) at 351 nm and a negative one ($\Delta\varepsilon$ −3.6) at 329 nm. The former appears in the region of a weak, structureless electronic absorption and is likely to originate from the $n-\pi^*$ transition (I in Table 2). The latter falls in the

  0947-6539/02/0811-2490 $ 20.00+.50/0 *Chem. Eur. J.* **2002**, *8*, No. 11

region of a UV maximum at 322 nm ($\varepsilon = 2600$), which is due to a z-polarized $\pi-\pi^*$ transition (III). A very weak Cotton effect at 307 nm ($\Delta\varepsilon +0.4$) is also observed, which corresponds to a UV maximum at 310 nm ($\varepsilon = 3100$) originating from the y-polarized $\pi-\pi^*$ transition (IV). A CD maximum at 285 nm ($\Delta\varepsilon +2.1$) has no corresponding UV maximum, but falls in the region of the band V $\pi-\pi^*$ transition.

Analysis of the CD spectrum of unstrained cyclic trimer **5** (Figure 11) yields a wealth of data on the pyromellitdiimide electronic transitions. This is in contrast to the UV spectrum, which does not differ greatly from those of monomer **1b** or acyclic dimer **2b** or trimer **3** other than in the positions and intensities of the maxima. The main UV maximum ($\varepsilon =$ 137 500 at 233 nm), attributable to the z-polarized $\pi-\pi^*$ transition in the monomer, is blue-shifted (by about 7 nm) from the position of λ_{max} of **1b**. This is to be expected for the exciton energy system in cyclic trimers, in which the higher exciton state is allowed whereas the lower exciton state has (partly) forbidden character.[30]

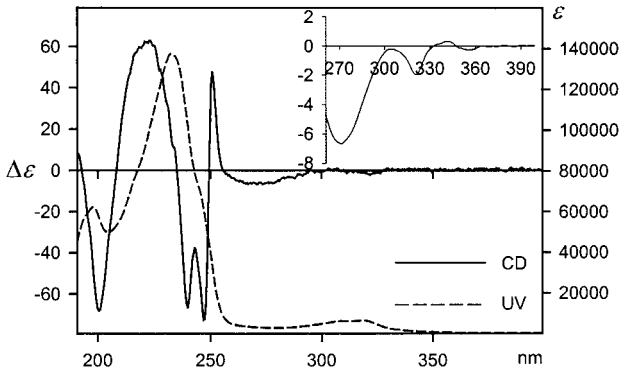

Figure 11. CD and UV spectra of **5** in acetonitrile (conditions as for Figure 9).

Cyclic trimer **5** belongs to the D_3 symmetry point group and, with respect to its absolute configuration, its structure can be regarded as equivalent to that of a tris-chelate metal complex of Δ configuration. The allowed $\pi-\pi^*$ transitions are either polarized in the direction of the C_3 axis (A_2 band, in-phase coupling) or in the plane perpendicular to the C_3 axis (E band, out-of-phase coupling). For the given absolute configuration of **5**, the E band Cotton effect is of lower energy and negative, while the A_2 band is of higher energy and positive. This principle, when applied to **5**, allows for a more complete experimental assignment of the electronic transitions in the pyromellitic chromophore, especially in the region 200–260 nm. In the aforementioned region, three pairs of exciton Cotton effects are seen. A positive couplet ($\Delta\varepsilon +46.3$ at 251 nm and $\Delta\varepsilon -72.5$ at 247 nm), attributable to transition VI (Table 2), is followed by a negative couplet ($\Delta\varepsilon -66.6$ at 240 nm and $\Delta\varepsilon +62.8$ at 223 nm) belonging to the main transition VII, and another positive couplet ($\Delta\varepsilon +62.8$ at 223 nm and $\Delta\varepsilon -68.1$ at 200 nm) of transition VIII, the lower energy Cotton effect of which apparently overlaps with the higher energy Cotton effect of transition VII. It is difficult to ascertain whether the sign sequence of the Cotton effects of **5** in the region 260–200 nm results from changes in energy ordering of the E and A_2 states for each transition, or, perhaps more likely, whether it is due to *hetero* coupling of the strong electric dipole allowed 233 nm transition VII with the transitions belonging to the adjacent bands VI and VIII. This coupling is likely to dominate over any *homo* coupling within the transitions VI and VIII. Circumstances favoring *hetero* couplings are the close energies of the transitions VI–VIII and the rigid structure of **5**. The latter feature is of particular importance since, in the case of **2b** and **3**, no significant *hetero* coupling comes into play due to the averaging effect of the spatial orientations of the y-polarized electric dipole transition moments caused by rotation about the pyromellitdiimide long axis. In any case, the sign sequence of the Cotton effects due to transitions polarized along the long (z) and short (y) axes in the individual pyromellitic chromophores should be opposite, as is observed for the short wavelength transitions of **5** (Table 2). At longer wavelengths, a Cotton effect is observed at 270 nm ($\Delta\varepsilon -6.7$), which corresponds to the very weak y-polarized transition V observed in the LD spectrum of **1b** in a stretched PVC film. Other CD bands detected for **5** (Figure 11, insert) are localized at 320 nm ($\Delta\varepsilon -2.0$), corresponding to transition III, along with two very weak $n-\pi^*$ Cotton effects ($\Delta\varepsilon +0.3$ at 342 nm and $\Delta\varepsilon -0.2$ at 355 nm), labeled as transitions II and I in Table 2.

Comparison with ab initio and semiempirical calculations: Due to the size of the molecules under consideration, it was only feasible to perform ab initio calculations of their UV and CD spectra at a low level of theory, namely including only the singly-excited configurations from a Hartree–Fock reference wavefunction (CIS[31]) and using the polarized double-zeta basis set (cc-pVDZ[32]). Therefore, the electron correlation effects in the excited states could not be accurately accounted for, and agreement with the experimental data is only moderate (as could have been expected). For the parent pyromellitdiimide **1a**, the ab initio calculated UV spectrum is dominated by two strong $\pi-\pi^*$ transitions (see Table 2). The first transition is computed to appear at $\lambda = 171$ nm, polarized along the long (z) axis of the molecule, whereas the second transition is predicted to appear at $\lambda = 160$ nm, polarized along the short (y) axis. The first transition corresponds to the strong UV absorption band observed for **1b** at $\lambda = 240$ nm, whereas the second transition could be assigned to the band shoulder observed either at about $\lambda = 250$ nm or at $\lambda =$ 220 nm. To account for the electron correlation effects, all the computed transition wavelengths were subsequently multiplied by an empirical scaling factor of 1.4 (as compared with 1.33 found in the previous study[11]). The ab initio calculated UV spectrum resembles that determined by the semiempirical INDO/S approach, although the ordering of some transitions is different. For example, the lowest-energy transition computed at the ab initio level is of $\pi-\pi^*$ character (B_{2u}), whereas INDO/S computation indicates a B_{3u} $n-\pi^*$ transition to be the lowest in energy. The experimental UV bands (I–VIII) are shown in Table 2 in the order corresponding to the symmetry-related transitions calculated by the INDO/S method.

The observed and calculated CD spectra of dimeric pyromellitdiimides **2a** and **4** are compared in Figures 9 and 10, respectively. The main features of the observed spectra are seen to be reproduced. The calculated CD spectra in the region 220–260 nm consist of several pairs of close-lying Cotton effects with opposite signs. In the case of **2a**, the low-energy component in each pair is negative in sign, as would be anticipated for the absolute spatial arrangement of the chromophores, regardless of the direction of polarization (y,z) of the two transitions. The spectra of the acyclic dimer **2a** and the cyclic dimer **4** are predicted to be different, as is indeed observed. However, for the reasons mentioned above, agreement with the experimental spectra can only be considered as qualitative.

Conclusion

We have prepared and characterized the acyclic and cyclic dimers and trimers of pyromellitdiimide connected by rigid *trans*-1,2-disubstituted cyclohexane spacers. LD and MCD measurements on pyromellitdiimide **1b** as well as CD spectral measurements on pyromellitdiimide dimers and trimers **2b**–**5** have provided complementary data on a number of transitions of the pyromellitdiimide chromophore. These include the n–π* transitions at the longer wavelength tail of the UV absorption, and up to six π–π* transitions that are polarized in the plane of the chromophore along one of the two symmetry axes (y,z). The most detailed assignment was possible on the basis of the CD/UV data of the chiral cyclic trimer **5**, the structure of which has been established through spectroscopic and X-ray diffraction studies, as well as by molecular modeling. Key to the assignments of the π–π* transitions was the sign of the exciton split Cotton effects, in conjunction with the exciton couplet due to the long-axis polarized intense π–π* transition at around 240 nm. The experimental results have been further supported by computations, either at the ab initio CIS/cc-pVDZ or semiempirical INDO/S level of theory. The computed transition pattern is in qualitative agreement with the experimental one, and corroborates the polarizations of the main π–π* transitions.

The data reported herein have allowed the first complete characterization of the electronic transitions of the pyromellitdiimide chromophore. They should find valuable use in allowing stereochemical assignments of pyromellitdiimide-based molecules, systems of interest in both biological and materials science contexts, by providing information on either the conformation or the absolute configuration. Work along these lines is in progress in this laboratory.

Experimental Section

General methods: Unless stated otherwise, NMR spectra were recorded at ambient temperature on a Varian XL300 instrument and are reported in ppm with respect to $(CH_3)_4Si$ ($\delta = 0$) as a reference. CD and UV spectra were measured on a JASCO 810 spectropolarimeter. Alternatively, UV spectra were recorded on a JASCO V-550 spectrophotometer. MS were measured with a 604 AMD Intectra spectrometer. All organic solvents were of spectrophotometric grade. Diimides **1b** and **2b** have been reported previously.[9]

X-ray diffraction studies of compounds 4 and 5: Diimide **4** crystallized from benzene as an inclusion compound with the formula $C_{32}H_{24}N_4O_8 \cdot C_6H_6$. $M_r = 670.66$, $T = 150$ K, triclinic, space group $P1$, $a = 6.917(1)$, $b = 7.569(2)$, $c = 15.812(3)$ Å, $\alpha = 82.91(3)$, $\beta = 81.64(3)$, $\gamma = 71.09(3)^\circ$, $V = 772.3(3)$ Å^3, $Z = 1$, $\rho_{calcd} = 1.442$ g cm^{-3}, $Mo_{K\alpha}$ radiation ($\lambda = 0.71073$ Å), $\mu = 0.10$ mm^{-1}, final R value 0.039 for 2885 observed reflections [$I > 2\sigma(I)$]. A crystal of approximate dimensions $0.40 \times 0.25 \times 0.15$ mm was used for data collection on a KM4 CCD diffractometer,[33], with a graphite crystal monochromator in the incident beam. θ_{max} was 26.37°, and the hkl ranges were −8/8, −5/9, and −19/19, respectively. Of the 6472 reflections collected, 3136 were unique ($R_{int} = 0.027$) and 2885 were considered as observed with $I > 2\sigma(I)$.

Diimide **5** crystallized from benzene as an inclusion compound with the formula $C_{48}H_{36}N_6O_{12} \cdot 3\,C_6H_6$. $M_r = 1123.15$, $T = 295$ K, hexagonal, space group $P6_3$, $a = b = 15.825$ Å, $c = 13.701(3)$ Å, $V = 2791.5(8)$ Å^3, $Z = 2$, $\rho_{calcd} = 1.255$ g cm^{-3}, $\rho_{exptl} = 1.223$ g cm^{-3}, $Cu_{K\alpha}$ radiation ($\lambda = 1.54178$ Å), $\mu = 0.717$ mm^{-1}, final R value 0.040 for 2691 observed reflections [$I > 2\sigma(I)$]. A crystal of approximate dimensions $0.4 \times 0.4 \times 0.4$ mm was used for data collection on a KM-4[34] diffractometer, with a graphite crystal monochromator in the incident beam. θ_{max} was 65.10°, and the hkl ranges were 0/18, −16/0, and −14/16, respectively. Of the 3394 reflections collected, 2959 were unique ($R_{int} = 0.016$), and 2691 were considered as observed with $I > 2\sigma(I)$.

The structures were solved by direct methods (SHELXS-86[35]) and refined by full-matrix least-squares by using SHELXL-97.[36] A Siemens Stereochemical Workstation was used to prepare the drawings.[22] Anisotropic thermal parameters were refined for all non-hydrogen atoms in the crystal of **4** and for most of the non-hydrogen atoms in the crystal of **5**. The hydrogen atoms were placed in calculated positions (C–H = 0.96 Å) and refined in a "riding model" with their U_{iso} values 1.2 times greater than U_{eq} of the atoms to which they were bonded. In the crystal of **5**, the benzene molecules situated on a threefold axis are disordered over four distinct positions in such a way that the dominant contributor is oriented perpendicularly to the threefold axis, while the remaining three minor contributors are arranged parallel to this symmetry axis. The relative ratios of the major and minor components in the disorder model were 0.75:0.08 for one benzene molecule and 0.48:0.17 for the other. CCDC-172262 (**4**) and -172263 (**5**) contain the supplementary crystallographic data for this paper. These data can be obtained free of charge via www.ccdc.cam.ac.uk/conts/retrieving.html (or from the Cambridge Crystallographic Data Centre, 12 Union Road, Cambridge CB21EZ, UK; fax: (+44) 1223-336-033; or e-mail: deposit@ccdc.cam.ac.uk).

Linear dichroism (LD) and magnetic circular dichroism (MCD): For a description of the methodology and further references, see ref. [11].

Computational details: The equilibrium structures of the monomeric and dimeric pyromellitdiimides (**1a**, **2a**, **4**) in their ground electronic states were determined by the density functional theory (DFT) approach. The hybrid method B3LYP,[37] and a one-particle basis set of double-zeta quality (cc-pVDZ)[32] were applied. The structures thus determined were used to compute the transition energies and intensities of the excited electronic states by the ab initio (CIS[31]) and semiempirical (INDO/S-CI[38]) configuration interaction methods. In the CIS approach, the calculations included all singly-excited configurations within the active space, which consisted of all the occupied valence and virtual molecular orbitals of a Hartree–Fock reference wavefunction. In the INDO/S-CI calculations, all the singly-excited configurations with energies up to 12 eV were taken into account. The calculations were performed using the Gaussian-98 suite of programs.[39]

Trimeric pyromellitdiimide 3: A solution of pyromellitic anhydride (55 mg, 0.25 mmol) in DMF (1 mL) was slowly added to a solution of (1*R*,2*R*)-1,2-diaminocyclohexane (57 mg, 0.5 mmol) in DMF (1 mL). The mixture was stirred overnight at room temperature and was then added to a solution of pyromellitic anhydride (109 mg, 0.5 mmol) in DMF (1 mL). After stirring overnight at room temperature, cyclohexylamine (50 mg, 0.5 mmol) was added and the mixture was heated at 130 °C for 3 h. After dilution with cold water, the crude mixture of products was separated by filtration and subjected to column chromatography on silica gel eluting with CH_2Cl_2/5% AcOEt. Compound **3** was obtained as a colorless solid, yield 5%; m.p. >360 °C; IR (KBr): $\tilde{\nu} = 1711$, 1769 cm^{-1} (C=O); ^{1}H NMR ($CDCl_3$):

  0947-6539/02/0811-2492 $ 20.00+.50/0 *Chem. Eur. J.* **2002**, *8*, No. 11

$\delta = 1.25-1.38$ (m, 10H), 1.42–1.52 (m, 2H), 1.64–1.72 (m, 6H), 1.85–1.94 (m, 10H), 2.08–2.22 (m, 4H), 2.46 (m, 4H), 4.13 (m, 2H), 4.92 (m, 4H), 8.01–8.18 (br m, 6H); UV (dioxane): λ_{max} (ε) = 236 (76100), 323 nm (3700); FAB MS: *m/z*: 973.0 [M^++1].

Cyclic dimeric diimide 4: In a representative experiment, (1*R*,2*R*)-1,2-diaminocyclohexane (114 mg, 1 mmol) was heated with pyromellitic anhydride (218 mg, 1 mmol) in DMF (5 mL) at 50 °C for 1 h. Ac_2O (0.5 mL) and NEt_3 (0.5 mL) were then added, and the mixture was stirred overnight at room temperature. It was subsequently concentrated to dryness in vacuo, the residue was redissolved in dichloromethane, and the resulting solution was extracted with 1N HCl, 1M $NaHCO_3$, and H_2O. The dichloromethane layer was dried and concentrated, and the residue was subjected to column chromatography on silica gel eluting with dichloromethane. Cyclic diimide **4** was obtained as a colorless solid, yield 16%; m.p. >360 °C; IR (KBr): $\tilde{\nu}$ = 1733, 1781 cm^{-1} (C=O); ^{1}H NMR ($CDCl_3$): δ = 1.50–1.75 (m, 4H), 1.95–2.35 (m, 12H), 4.89 (m, 4H), 7.86 (s, 4H); FAB MS: *m/z*: 593.1 [M^++1].

Cyclic trimeric diimide 5: (1*R*,2*R*)-1,2-Diaminocyclohexane (114 mg, 1 mmol) and pyromellitic anhydride (218 mg, 1 mmol) were refluxed in acetic acid (5 mL) for 4 h. The solvent was removed in vacuo and the residue was digested by refluxing with dichloromethane for 1 h. Polymeric material (220 mg) was removed from the dichloromethane extract by filtration and the filtrate was concentrated to dryness. Column chromatography of the residue on silica gel eluting with CH_2Cl_2/1% AcOEt afforded cyclic diimide **5** as a colorless solid; yield 11%; m.p. >360 °C; IR (KBr): $\tilde{\nu}$ = 1728, 1774 cm^{-1} (C=O); ^{1}H NMR ($CDCl_3$): δ = 1.50–1.65 (m, 6H), 1.90–2.15 (m, 18H), 5.18 (m, 6H), 8.04 (s, 6H); FAB MS: *m/z*: 889.1 [M^++1].

Acknowledgements

We thank Jakub Grajewski for computational assistance. Ab initio calculations were performed at the Poznan Supercomputer Center (PCSS). This work was supported by the Committee for Scientific Research (KBN), grant no. 3T09A 025 17, and the Swedish Science Research Council.

[1] a) G. D. Storrier, S. B. Colbran, *J. Chem. Soc. Dalton Trans.* **1996**, 2185; b) D. G. Hamilton, J. K. G. Sanders, J. E. Davies, W. Clegg, S. J. Teat, *Chem. Commun.* **1997**, 897; c) D. G. Hamilton, J. E. Davies, L. Prodi, J. K. M. Sanders, *Chem. Eur. J.* **1998**, *4*, 608; d) D. G. Hamilton, N. Feeder, S. J. Teat, J. K. M. Sanders, *New J. Chem.* **1998**, 1019; e) J. G. Hansen, N. Feeder, D. G. Hamilton, M. J. Gunter, J. Becher, J. K. M. Sanders, *Org. Lett.* **2000**, 449.

[2] K. Kishikawa, S. Tsubokura, S. Kohmoto, M. Yamamoto, *J. Org. Chem.* **1999**, *64*, 7568.

[3] G. P. Wiederrecht, W. A. Svec, M. R. Wasielewski, T. Galili, H. Levanon, *J. Am. Chem. Soc.* **2000**, *122*, 9715.

[4] a) A. Osuka, T. Okada, S. Taniguchi, K. Nozaki, T. Ohno, N. Mataga, *Tetrahedron Lett.* **1995**, *36*, 5781; b) A. Osuka, S. Marumo, Y. Wada, I. Yamazaki, T. Yamazaki, Y. Shirakawa, Y. Nishimura, *Bull. Chem. Soc. Jpn.* **1995**, *68*, 2909; c) A. Osuka, S. Nakajima, T. Okada, S. Taniguchi, K. Nozaki, T. Ohno, I. Yamazaki, Y. Nishimura, N. Mataga, *Angew. Chem.* **1996**, *108*, 98; *Angew. Chem. Int. Ed. Engl.* **1996**, *35*, 92; d) A. Osuka, S. Marumo, N. Mataga, S. Taniguchi, T. Okada, I. Yamazaki, Y. Nishimura, T. Ohno, K. Nozaki, *J. Am. Chem. Soc.* **1996**, *118*, 155; e) H. Shiratori, T. Ohno, K. Nozaki, A. Osuka, *Chem. Commun.* **1999**, 2181; f) H. Shiraton, T. Ohno, K. Nozaki, I. Yamazaki, Y. Nishimura, A. Osuka, *J. Org. Chem.* **2000**, *65*, 8747.

[5] T. Nagata, *Bull. Chem. Soc. Jpn.* **1991**, *64*, 3005.

[6] a) C. A. Hunter, J. K. M. Sanders, G. S. Beddart, S. Evans, *J. Chem. Soc. Chem. Commun.* **1989**, 1765; b) H. L. Anderson, C. A. Hunter, M. Nafees Meah, J. K. M. Sanders, *J. Am. Chem. Soc.* **1990**, *112*, 5780.

[7] a) J. H. Borkent, J. W. Verhoeven, Th. J. de Boer, *Chem. Phys. Lett.* **1976**, *42*, 50; b) H. A. Staab, S. Nikolic, C. Krieger, *Eur. J. Org. Chem.* **1999**, 1459.

[8] G. P. Wiederrecht, M. P. Niemczyk, W. A. Svec, M. R. Wasielewski, *J. Am. Chem. Soc.* **1996**, *118*, 81.

[9] J. Gawroński, M. Brzostowska, K. Kacprzak, H. Kołbon, P. Skowronek, *Chirality* **2000**, *12*, 263.

[10] F. Kazmierczak, K. Gawrońska, U. Rychlewska, J. Gawroński, *Tetrahedron: Asymmetry* **1994**, *5*, 527.

[11] J. Gawroński, F. Kazmierczak, K. Gawrońska, U. Rychlewska, B. Nordén, A. Holmen, *J. Am. Chem. Soc.* **1998**, *120*, 12083.

[12] J. Gawroński, M. D. Rozwadowska, F. Kazmierczak, *Pol. J. Chem.* **1994**, *68*, 2279.

[13] P. Skowronek, J. Gawroński, *Tetrahedron: Asymmetry* **1999**, *10*, 4585.

[14] P. Skowronek, J. Gawroński, *Tetrahedron Lett.* **2000**, *41*, 2975.

[15] A. Kawamura, N. Berova, V. Dirsch, A. Mangoni, K. Nakanishi, G. Schwartz, A. Bielawska, Y. Hannun, Y. Kitagawa, *Bioorg. Med. Chem.* **1996**, *4*, 1035.

[16] Cyclic dimeric and trimeric structures, analogous to **4** and **5**, are not uncommon among fully carboxylic compounds; see, for example: a) T. Nishinaga, T. Kawamura, K. Komatsu, *J. Org. Chem.* **1997**, *62*, 5354; b) M. Chakraborty, C. A. Tessier, W. J. Youngs, *J. Org. Chem.* **1999**, *64*, 2947; c) J. M. Kehoe, J. H. Kiley, J. J. English, C. A. Johnson, C. Petersen, M. M. Haley, *Org. Lett.* **2000**, 969; d) W. B. Wan, S. C. Brandt, J. J. Pak, M. M. Haley, *Chem. Eur. J.* **2000**, *6*, 2044. Chiral triangular compounds such as cycloveratrylenes (J. Canceill, A. Collet, J. Gabard, G. Gottarelli, G. P. Spada, *J. Am. Chem. Soc.* **1985**, *107*, 1299), cyclophanes (S. Anderson, U. Neidlein, V. Gramlich, F. Diederich, *Angew. Chem.* **1995**, *107*, 1722; *Angew. Chem. Int. Ed. Engl.* **1995**, *34*, 1596), and trimetallic complexes with bridging ligands (R.-D. Schnebeck, L. Randaccio, E. Zangrando, B. Lippert, *Angew. Chem.* **1998**, *110*, 130; *Angew. Chem. Int. Ed.* **1998**, *37*, 119; T. Habereder, M. Warchhold, H. Nöth, K. Severin, *Angew. Chem.* **1999**, *111*, 3422; *Angew. Chem. Int. Ed.* **1999**, *38*, 3225) have been extensively studied.

[17] For a definition of chiral *C* and *S* conformers, see: J. Gawroński, K. Gawrońska, K. Kacprzak, *Chirality* **2001**, *13*, 322. For an alternative *syn*/*anti* assignment, see: C. Degenhardt, D. B. Shortell, R. D. Adams, K. D. Shimizu, *Chem. Commun.* **2000**, 929.

[18] The ^{1}H NMR spectrum of **2b** recorded at 243 K features two sharp singlets of equal intensity due to the aromatic protons; see ref. [17].

[19] S. R. Koropoju, P. S. Zacharias, *Chem. Commun.* **1998**, 1267.

[20] J. Gawroński, H. Kołbon, M. Kwit, A. Katrusiak, *J. Org. Chem.* **2000**, *65*, 5768.

[21] M. Chadim, M. Budešinský, J. Hodačová, J. Závada, P. C. Junk, *Tetrahedron: Asymmetry* **2001**, *12*, 127.

[22] Stereochemical Workstation Operation Manual, Release 3.4, Siemens Analytical X-ray Instruments, Inc., Madison, Wisconsin (USA), **1989**.

[23] I. V. Bulgarovskaya, L. A. Novakovskaya, Yu. G. Federov, Z. V. Zvonkova, *Kristallografiya* **1976**, *21*, 515.

[24] D. G. Hamilton, D. E. Lynch, K. A. Byriel, C. H. L. Kennard, *Aust. J. Chem.* **1997**, *50*, 439.

[25] I. V. Bulgarovskaya, L. A. Smelyanskaya, Yu. G. Federov, Z. V. Zvonkova, *Kristallografiya* **1977**, *22*, 184.

[26] D. G. Hamilton, D. E. Lynch, K. A. Byriel, C. H. L. Kennard, J. K. M. Sanders, *Aust. J. Chem.* **1998**, *51*, 1998.

[27] E. L. Eliel, S. H. Wilen, *Stereochemistry of Organic Compounds*, Wiley, New York, **1994**, p. 686.

[28] B. Nordén, R. Håkansson, P. B. Pedersen, E. W. Thulstrup, *Chem. Phys.* **1978**, *33*, 355.

[29] B. Nordén, *Appl. Spectrosc. Rev.* **1978**, *14*, 157.

[30] M. Kasha, H. R. Rawls, M. A. El-Bayoumi, *Pure Appl. Chem.* **1965**, *11*, 371.

[31] J. B. Foresman, M. Head-Gordon, J. A. Pople, M. J. Frisch, *J. Phys. Chem.* **1992**, *96*, 135.

[32] T. H. Dunning, Jr., *J. Chem. Phys.* **1989**, *90*, 1007.

[33] KM4CCD Software, Version 1.163, Kuma Diffraction Instruments GmbH, Wrocław (Poland), **1999**.

[34] KM-4 Diffractometer Operating System and Data Reduction Software, Kuma Diffraction, Wrocław (Poland), **1991**.

[35] G. M. Sheldrick, *Acta Crystallogr. Sect. A* **1990**, *46*, 467.

[36] G. M. Sheldrick, SHELXL-97, University of Göttingen, **1997**.

[37] A. D. Becke, *J. Chem. Phys.* **1993**, *98*, 5648.

[38] J. Ridley, M. C. Zerner, *Theor. Chim. Acta* **1973**, *32*, 111.

[39] Gaussian 98 (Revision A.9), M. J. Frisch, G. W. Trucks, H. B. Schlegel, G. E. Scuseria, M. A. Robb, J. R. Cheeseman, V. G. Zakrzewski, J. A. Montgomery, R. E. Stratmann, J. C. Burant, S. Dapprich, J. M.

Millam, A. D. Daniels, K. N. Kudin, M. C. Strain, O. Farkas, J. Tomasi, V. Barone, M. Cossi, R. Cammi, B. Mennucci, C. Pomelli, C. Adamo, S. Clifford, J. Ochterski, G. A. Petersson, P. Y. Ayala, Q. Cui, K. Morokuma, D. K. Malick, A. D. Rabuck, K. Raghavachari, J. B. Foresman, J. Cioslowski, J. V. Ortiz, B. B. Stefanov, G. Liu, A. Liashenko, P. Piskorz, I. Komaromi, R. Gomperts, R. L. Martin, D. J. Fox, T. Keith, M. A. Al-Laham, C. Y. Peng, A. Nanayakkara, C. Gonzalez, M. Challacombe, P. M. W. Gill, B. G. Johnson, W. Chen, M. W. Wong, J. L. Andres, M. Head-Gordon, E. S. Replogle, J. A. Pople, Gaussian, Inc., Pittsburgh PA, **1998**.

Received: October 22, 2001 [F3631]

  0947-6539/02/0811-2494 $ 20.00+.50/0